7. The backward detectors specifically the SPACAL calorimeter and some smaller units have to be rolled out of the solenoid, which is connected with major uncabeling work. This operation has been done every shut down so far.
8. **At this point the removal of the central beam pipe with the interaction magnets and Silicon trackers can start.**
9. The beam pipe forming one unit together with the interaction magnets is pushed from the +z side (forward direction) through the experiment and whenever a segment appears outside the central tracker, flanges are opened and the segments are moved out. This is the most critical part of the whole operation. The pushing procedure has been applied before, when H1 installed beam pipes and all tools were available. This time, however, the additional weight of the magnets has to be considered and a more advanced rolling system has to be designed.

The above procedure describes the access to the central beam pipe with the interaction magnets. For reinstallation the scheme is reversed. Different submodules are flanged together at the +z side and then pushed through H1 to the -z side.

The time estimated for a complete cycle with opening and closing the experiment is estimated to take about 8 weeks assuming 8 hours working days and 5 days per week. Between 2 and 3 weeks are needed for opening, and at least 5 weeks for closing, recabelling and testing.

In case access is required to the forward trackers or the central drift chambers, H1 has to be moved to the parking position. There essentially the same scheme will be pursued with the only difference that some of the operations are easier because of the better accessibility. The procedure described above assumes warm magnets in the interaction region. For superconducting coils we may follow essentially the same route except that additional time will be required for warming up and cool down. Disconnecting the cryo lines will not present a technical problem, because experience exists in H1 from disconnecting the main solenoid from the Helium supply. Also the extra time required is negligible compared with the total length down time needed for the complete operation.

10 Vacuum System

10.1 Specification of the Vacuum System in the IR

The background rate in the detector and the first level trigger rate of the data acquisition are determined by the beam conditions and by interactions of the electron and proton beams with the residual gas inside the vacuum system.

A residual gas pressure of $\lesssim 10^{-9}$ mbar is required at the interaction region and upstream of the proton beam for good running conditions. The pressure in the common vacuum system is mainly determined by the desorption induced by synchrotron radiation, thermal desorption, the available pumping speed and the conductance of the vacuum chambers. Thermal desorption due to higher order mode losses of the electron beam are small, provided there is adequate cooling of the vacuum chambers.

Local pressure maxima are expected at two different positions. The synchrotron radiation absorber at the septum will be hit by 2 kW of synchrotron radiation, which will lead to increased synchrotron radiation induced desorption and thermal desorption, which requires dedicated pumping (see section **??**). Another pressure maximum will occur at the interaction region, since there is no space for any pumping.

Absolute specifications of the requirements of the vacuum system are difficult to make, because the desorption rate, which decreases as a function of the integrated stored electron current in HERA, and the gas composition are not well known. In addition, the pumping speed of several pumps, e.g. Ti sublimation pumps or non-evaporable getter pumps, varies as a function of the sorped gas quantity. It it however useful to compare the layout of the new interaction region with the present vacuum system. Although the comparison is done with the present ZEUS interaction region (IR), the results and design consideration also apply for the H1 IR. In case of ZEUS, the pumping is provided by two ion getter and two Ti sublimation pumps located at z = + 4.6 m, four Ti sublimation pumps and two ion getter pumps located at z = − 4.0 m and z = − 5.5 m, respectively.

Assuming a cylindrical beam pipe of radius r and two pumps separated by a distance l, the pressure at the interaction region is given by:

$$p_{IR} = p_0 + \Delta p = \dot{q}\, 2\pi\, r\, l \left(\frac{1}{S} + \frac{1}{8} \frac{1}{C} \right) ,$$

where $\dot{q}$ is the specific desorption rate, S is the pumping speed and C the conductance of the beam pipe. p_0 is the pressure at both pumps. The pressure at the interaction region is given in table 32 for an initial specific desorption rate of $\dot{q} = 10^{-10} mbar\, l/s/cm^2$ and pumping speeds of $S_{H_2} = 1000\, l/s$ and $S_{H_2O} = 500\, l/s$ after activation of the Ti sublimation pumps. An average diameter of 10 cm was used to calculate the pressure for the present beam pipe. The pressure

Vacuum Pressure at IP (no integrated pumps)						
			p_0(mbar)		p_{IP}(mbar)	
	d (cm)	l (m)	H_2	H_2O	H_2	H_2O
present IP	10	8.7	2.7 10^{-9}	5.5 10^{-9}	9.1 10^{-9}	2.5 10^{-8}
new IP	4	11.4	1.4 10^{-9}	2.9 10^{-9}	7.0 10^{-9}	2.1 10^{-7}

Table 32: Vacuum pressure at the IP with no integrated pumps. The distance between the pumps on either side of the IP is 8.7 m with an average beam pipe diameter of 100 mm and 11.4 m (average diameter of 40 mm) for the present IR and the upgrade, respectively.

for the new interaction region was calculated in case the pumps are located at z = ± 5.7 m, i.e. downstream of both combined function magnets. An averaged beam pipe diameter of 4 cm was assumed, including the beam pipes inside both magnets on either side of the IP. For this arrangement, the pressure at the IP would be one order of magnitude higher than at the present IP, which would clearly deteriorate the background conditions of the experiment.

Similarly, the conductance of the beam pipe between the pump and the central beam pipe can be compared to the present design. The conductance of the present forward and rear ZEUS beam pipes are 66 l/s and 30 l/s, respectively, whereas it is only about 2 l/s for the beam pipe of both normal conducting combined function magnets (Rev 1). Beam pipe cross sections of 40 × 28 mm and 76 × 36 mm were used for the first and second combined function magnets.

Both estimates show that pumping at ± 5.7 m from the interaction point is insufficient. It is indispensable to position pumps close to the IP. In principle, there are two solutions: an integrated ion getter pump as part of the central beam pipe inside the magnetic field of the detector solenoid and distributed pumps inside the magnets. The integrated ion getter pump is however excluded because of the lack of available space. It would also add additional dead material in front of the calorimeter. Distributed pumps can be integrated in the magnet vacuum chambers as shown in Fig. 78. The stray magnetic field of the first combined function magnet is only about 0.04 T at the pumping channel, and thus insufficient for an integrated ion getter pump with reasonable cell size.

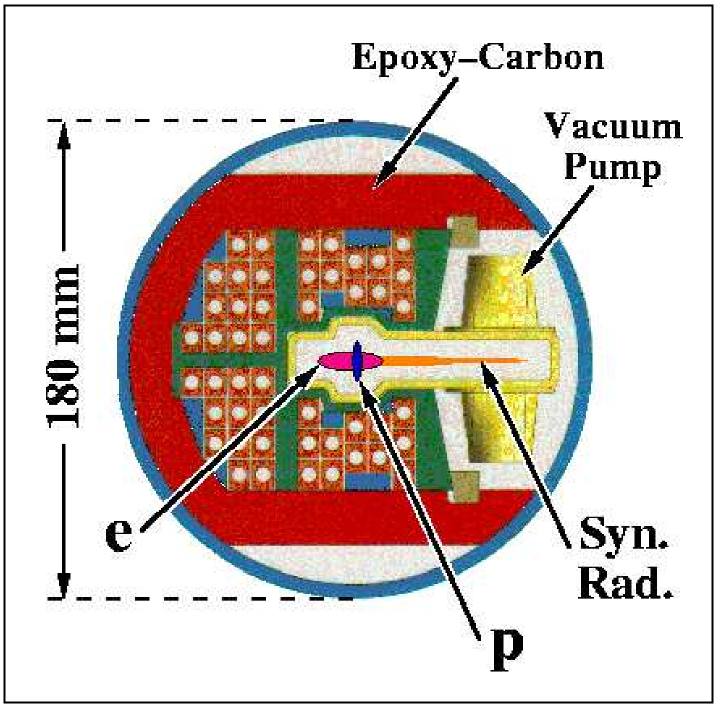

Figure 78: QG Magnet Schematic showing possible vacuum pump location.

It is planned to use non-evaporable getter pumps (NEG pumps) inside the vacuum chambers of the combined function magnets. NEG pumps consist of a zirconium/aluminium alloy, which acts as the active getter material. We are planning to use the St101 material manufactured by SAES GETTERS [1]. The zirconium/aluminium alloy is supported by a 15 mm wide konstantan ribbon. The support of the NEG pump will be similar to the design, which is presently in preparation for the HERA electron machine. One 15 mm wide ribbon will be installed in the lower and upper pumping channels of the vacuum chamber as shown in Fig. 78. The getter material is activated by heating to a temperature of 750° C for a few minutes. After activation the pumping speed saturates as a function of the sorbed gas quantity. The getter material has to be regenerated when the pumping is no longer sufficient. In case of CO and CO_2, the pumping is reduced to 50 l/s for a 1 m long, 30 mm wide strip (or two 15 mm wide strips) after a gas load of 0.17 mbar l [2]. Assuming an initial specific desorption rate of 10^{-10} mbar l/s/cm^2, the NEG pump has to be regenerated after 2 days. The time between regenerations increases to 200 days at a specific desorption rate of 10^{-12} mbar l/s/cm^2.

A power of 2.4 kW in needed in order to heat both NEG pumps (two 15 mm wide ribbons of 2 m length) to 750° C. The beam pipe is cooled using water cooling pipes as indicated in

Fig. 78. A moderate water flow velocity of 1 m/s is needed for an inner cooling pipe diameter of 6 mm and a temperature increase of 20° C.

Ion getter pumps located downstream of the combined function magnets are still necessary, since NEG pumps do no pump inert gases.

In case of superconducting magnets at the IP (Rev2), it is planned to have the beam pipe inside the superconducting magnets at a temperature of 70 K, as described in section **??**. The cold beam pipe will act as a cryo pump. There is no space and no need for a pumping channel with an integrated pump.

References

[1] SAES GETTERS S.p.A., 20151 Milano, Italy

[2] U. Schneekloth, DESY M-81/25 (1981).

10.2 The Vacuumsystem of the e-Ring (Kouptsidis)

10.2.1 Beam Pipes and Bellows

10.2.2 Pumping System

10.3 The Vacuum System of the Proton Ring

The electron and proton beams are separated at the septum magnets QM located at about 11 m from the IP. However, the distance of the two beams in the drift section right after the septum and within the following magnets is too small (≈ 20 mm) to install separate flanges for the electron and proton beam pipe. The separation of the proton and electron vacuum system will therefore be done behind the dipole magnet BO, which includes the last absorber, at about 28 m, where flanges and valves can be easily installed. The layout of the combined chambers up to this separation point are described elsewhere (see section 10.2).

10.3.1 Beam Pipes and Bellows

In the present layout, the proton lattice will be modified up to ± 60 m around the IP. This implements changing the vacuum chambers accordingly.

In order to minimize cost and manpower, the vacuum chambers of the present machine will be reused or modified whenever possible. For example the QR magnets will be moved to different locations. The distance between neighbouring magnets will be kept the same as in the present layout, such that the existing vacuum chambers including pump units can be used again.

In the present state of the project the details of the vacuum chambers have not been fixed.

10.3.2 Pumping System

The pumping of the warm sections of the HERA-proton ring is done by titanium sublimation pumps of 1000 l/s pumping speed supplemented with small (60 l/s) ion getter pumps. The pumps are mounted to circular vacuum chambers, which are installed sideways to the beam vacuum chamber. The profile of the beam chambers through the pump units is kept using slotted grids. The pump units are installed every 4 m resulting presently in an average pressure of a few times 10^{-10} mbar in the warm sections of HERA. The distance of pumping units will be kept the same for the new lattice.

To allow the installation of the vacuum chambers and to compensate changes in length each pump unit is equipped with a short bellows section along the beam pipe.

10.4 Synchroton Absorber system (Kouptsidis)

10.4.1 Requirements(Pitzl)

10.5 Cooling of the Synchrotron Radiation Absorbers.

The electron beam passing through the magnets in the interaction region is a strong source of synchrotron radiation. At 30 GeV and 58 mA the total radiated power (both sides) is 25 kW. Absorbers placed between 11 m and 27 m from the interaction point absorb 21 kW, the rest is passed on and absorbed at larger distances. The biggest power density and the biggest heat load will appear on the nearby set of absorbers up to 27 m, and only they will be treated.

Fig. 79 shows the arrangement of absorbers. They partially shield each other. Those which receive a non negligible amount of radiation are listed in table 33.

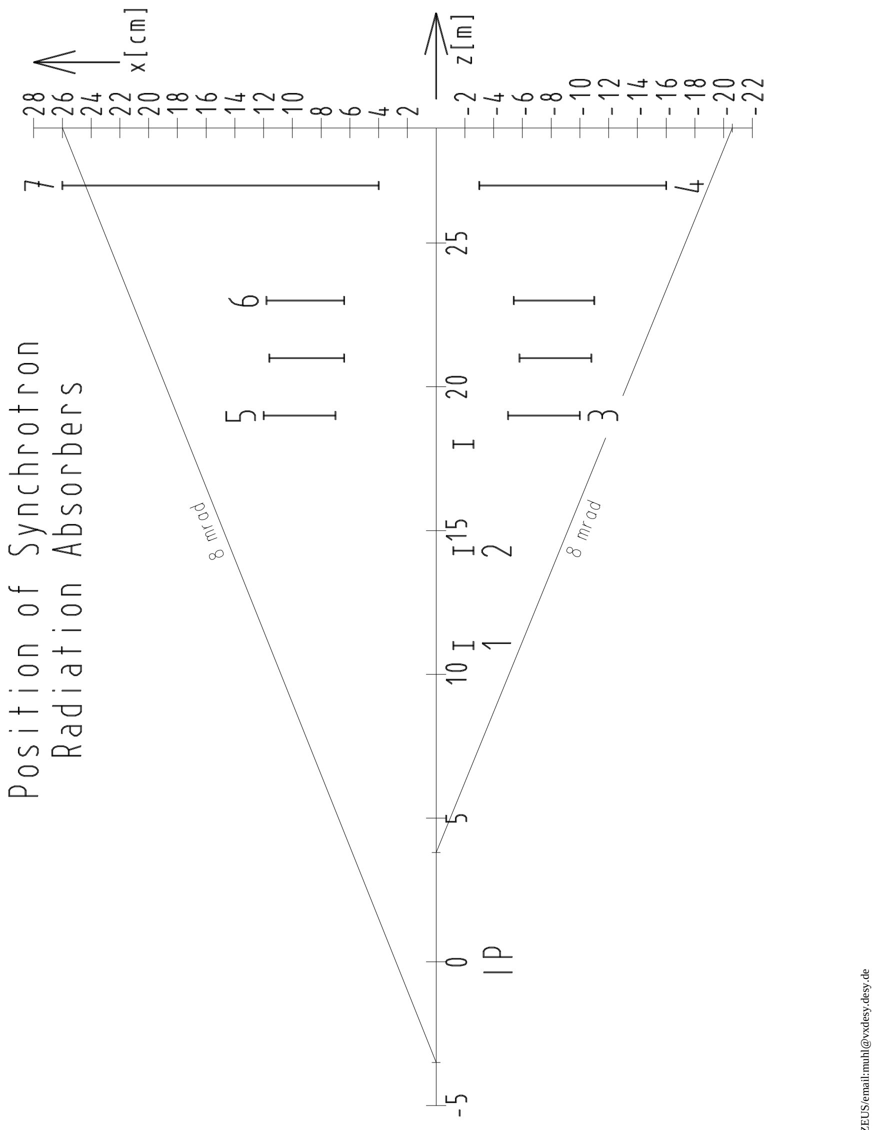

Figure 79: Position of synchrotron radiation absorbers.

absorber Nr.	distance (m)	abs.width (cm)	Power (kW)	power density (kW/cm)	σ (mm)
1	11	1.3	2.0	1.5	0.8
2	18	0.8	0.6	0.75	1.2
3	19	5.0	6.3	1.3	1.3
4	27	1.0	0.8	0.8	2.0
5	19	5.0	4.4	0.9	1.3
6	23	2.0	1.0	0.5	1.5
7	27	11.4	6.5	0.6	0.3

Table 33: Synchrotron radiation power on absorbers.

The individual absorbers are explained below:

1. Absorbers 1-4 are on the electron side, absorbers 5-7 are on the proton side. Their distances from the IP, their horizontal width, the power and linear power density and the vertical height (σ) of the radiation fan are given. The heights are estimated averages.
2. Absorber 1 is at the septum. It has the largest power density and a rather small beam height, and therefore appears the most critical.Its cooling will be discussed in some detail.
3. Absorbers 5 and 6 are inside magnets QN. They could be avoided if these quads have their coils split at the proton side to let the radiation fan pass through. In this case the power on absorber 7 will be larger (11.5 kW), spread over 20 cm.

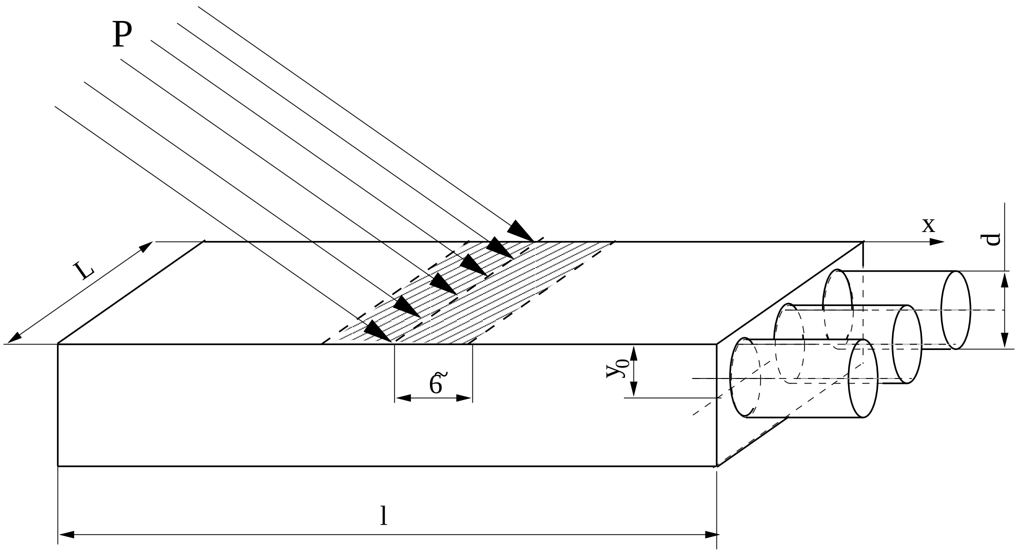

Figure 80: Sketch of the synchrotron radiation absorbers in front the septum magnet.

Fig 80 shows a sketch of absorber 1. It is made of copper and has to be water cooled. Three water pipes of 3 mm diameter are placed close to the surface. The temperature at the surface is given by the linear power density, the width of the radiation fan, the distance of the cooling pipes to the surface and the ability of the cooling pipes to absorb the power. The latter requirement is rather critical; it requires a large flow velocity of the cooling water.
The temperature difference T between the hottest point on the surface and the temperature of the cooling water is given by:

$$T = T_c + \Delta T$$

T_c is the temperature difference between the surface of the absorber and the surface of the cooling pipes, and ΔT is the temperature difference between the surface of the cooling pipe and the cooling water. If one replaces the cooling pipes by a plane with a constant temperature at a distance y_0 from the absorber surface, the problem can be solved analytically:

$$T_c(x) = \lim_{\Delta y \to 0} \frac{P}{L \cdot k} \frac{1}{4\sqrt{2}\pi^{3/2}} \int_{-\infty}^{\infty} e^{-\xi^2/2\sigma^2} \ln \frac{(2y_0 - \Delta y)^2 + (x-\xi)^2}{\Delta y^2 + (x-\xi)^2} d\xi$$

P=incident power, L= (horizontal) length of absorber, k=thermal conductivity of copper, σ=width of radiation fan, x=distance from the center of the radiation fan, y_0=distance between surface of absorber and cooling plane.

The equation for T_c was evaluated for the septum absorber 1 with the data from table 33, and with $y_0 = 5\,mm$ for the distance between the absorber surface and the cooling plane. Fig. 81 shows the temperature difference T_c for the hottest point on the surface, as a function of σ, the width of the radiation fan.
Using a width of $\sigma = 0.8\,mm$ from table 33, one obtains a temperature difference of 187° C. To reduce this high temperature, the incident radiation has to be distributed over a larger surface. This is achieved by choosing a grazing angle of incidence on the absorber. Using an angle of 50 mrad, the width becomes $\sigma/0.05 = 16\,mm$, and the temperature difference is reduced to 45° C.
This increase of the area of the incident radiation is even more important for the heat transfer to the cooling water. The heat transfer into the cooling water of a pipe is given by the following formula:

$$P = \frac{k_w \cdot N_m \cdot A}{D} \cdot \Delta T,$$

where $k_w = 0.6$ W/mK is the thermal conductivity of water.

$$N_m = 0.032 Re^{0.8} P_r^{0.37} \left(\frac{D}{l}\right)^{0.054}$$

The Reynolds number Re is

$$Re = \frac{vD}{\nu},$$

where v is the velocity, D the diameter of the pipe, ν the viscosity, and P_r Prandtl's number =7. $A = \pi D l$ is the surface area of the pipe, with length l. ΔT is the temperature difference between the cooling water and the wall, required to get the power P into the water.

In order to get a small temperature difference, Re and l have to be chosen large, i.e. a large flow velocity of the water and a large length of the pipe are of advantage. The following numerical values have been chosen:

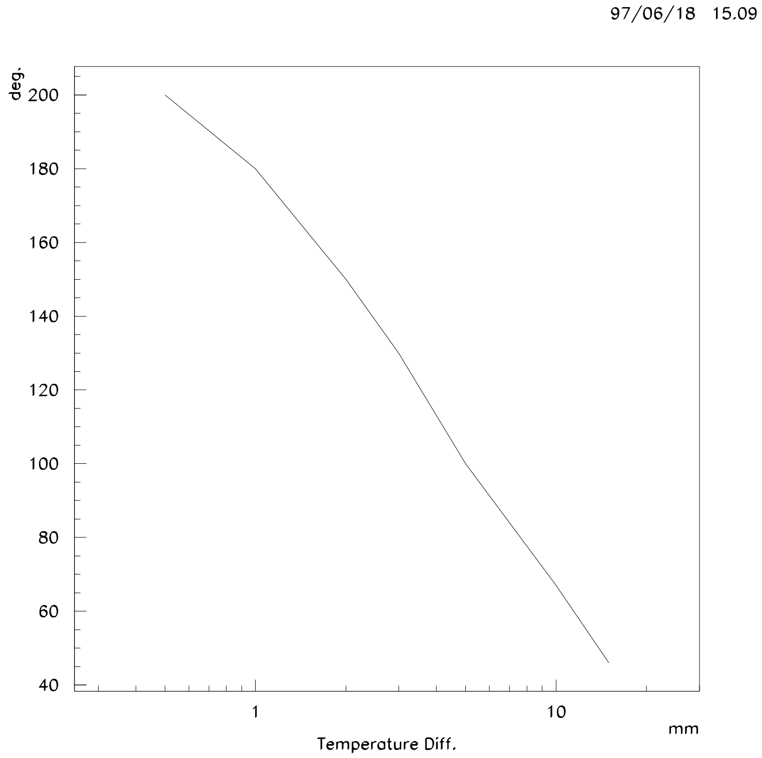

Figure 81: Temperature difference T_c for the hottest point on the surface as a function of σ, the width of the radiation fan.

v=7 m/s ,$\nu = 10^{-6}\, m^2$/s, D=3 mm, Re=20,000, l=2.5 cm ,P=2 kW.
Assuming that the heat load is distributed over 3 pipes, one obtains a temperature difference of $\Delta T = 90°$ C.

The temperature of the hottest spot on the surface of the absorber is therefore $45 + 90 \approx 135°$ C above the temperature of the cooling water. The required flow of water at 7 m/s should not be too difficult to achieve, since the pipes can be rather short. A pressure of 0.5-1.0 bar should suffice. The rise in water temperature will be about 3° C.

10.6 Mechanical Design and Layout (Kouptsidis)

10.7 Impedance Considerations for the Rev1 Design

Impedance calculations were carried out for the Beam Tube of the Interaction Region at ZEUS using the MAFIA programs [1]. Both wakefield (time domain), and resonant field (frequency domain) calculations were made. In the frequency domain the resonant fields were calculated for each mode, these fields can then be used to obtain the loss parameter, shunt impedance and power loss. Assuming that only one mode will be excited at any one time, the maximum values give a good worst case estimate of the potential power loss. As the damping time of the wakefields is longer than the time between bunches, the loss, calculated from wakefields, does not give an *absolute* value of the power loss which can be expected. However it does give a good measure of comparison for different beam tube geometries and for different longitudinal bunch lengths.

10.7.1 Geometry

The section of beam tube which was modeled is the 3.2 meter long section around the ZEUS Interaction Point ($z = 0.0m$), which forms a resonant cavity due to the changes in cross section at either end. It was only necessary to model half the structure as it is symmetrical with respect to the x-z plane. This is not the only section which forms a cavity but it is the most critical, as cooling is particularly difficult there.

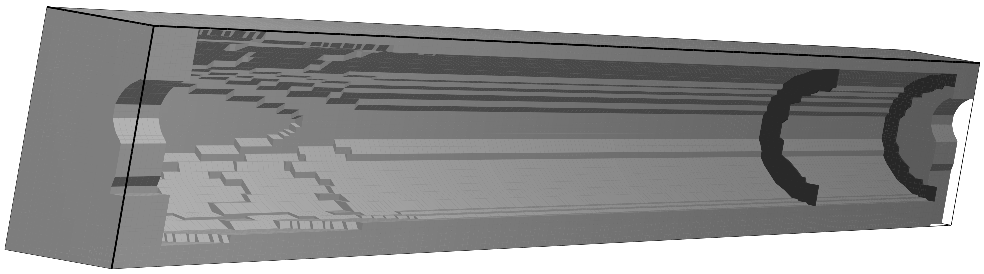

Figure 82: A foreshortened view of the inside of the proposed Zeus beam tube. The synchrotron light absorbers can be seen as dark arcs.

The geometry, proposed for the upgrade, consists of, from left to right, (see Figure 82):

- an elliptical beam tube inside the combined function magnet with lateral extension for synchrotron light, opening up into a conical section with an entry radius of $54\,mm$ at $z = -1.3\,m$ and an exit radius of $46.25\,mm$ at $z = -0.62\,m$;
- this is followed by a long cylindrical central beam pipe from $z = -0.62\,m$ to $z = 1.3\,m$;
- at $z = 1.3\,m$ there is a sudden change in cross section to an elliptical beam tube inside the other combined function magnet with a wider extension than that on the left hand side.
- Two synchrotron radiation absorbers will be positioned at $z = 0.75\,m$ and at $z = 1.3\,m$.

A second configuration was also investigated using an elliptical central beam pipe cross-section from $z = -1.3\,m$ to $z = 1.3\,m$. The height of the beam tube at the interaction point was $20\,mm$ as opposed to $46.25\,mm$ for the cylindrical cross-section, the width remained unchanged.

10.7.2 Time Domain

The damping time for a typical mode in this cavity with frequency= $2190.6 MHz$ and Q-factor= 23765 is given by

$$\tau = 2Q/\ \omega = 3.45 \mu sec\,(36 bunches).$$

As the bunch separation time is only 96 nanoseconds, this means that the wakefields from one bunch are still present when the next bunch arrives. The two extreme cases are when these fields are either in phase or out of phase with the wakefields from the next bunch. In the former case the losses accumulate while in the latter case they cancel. The losses drop dramatically with

Table 34: Variation of Longitudinal σ for Positrons/Electrons

Energy:	12 GeV	27.5 GeV	29.8 GeV
Voltage:	90 MV	110 MV	140 MV
Sigma:	3mm	12.3mm	13.4mm

the length of the bunch, so that maximum losses can be expected at injection. The longitudinal σ for positrons or electrons varies with beam energy as shown in Table 34.

In order to simulate the beam, the time domain program represents the bunch as a rigid longitudinal Gaussian charge distribution. For this geometry, 4mm is the smallest value of the σ of the distribution which could be calculated directly, as the extreme ratio of height to length of the beam tube begins to cause numerical problems. The 3mm bunch length was calculated in two halves. On the left hand side it is necessary to take the group velocity of the wakefields into account and to calculate to the point where the tail of the bunch has outstripped the wakefields, $z = 0.9\,m$. See Table 35 for a summary of the results of these calculations.

Table 35: The Single Pass Loss and the Maximum Total Resonant Power Loss for a mode for Cylindrical and Elliptical Beam Tubes

Beam Tube	Bunch Length	Single Pass Power Loss	Resonant Power Loss
Cylindrical			
	3mm	578+1292=1870 Watt	1993 Watt
	4mm	1338 Watt	1978 Watt
	7mm	597 Watt	1910 Watt
	8mm	493 Watt	1881 Watt
	13mm	203 Watt	1684 Watt
Elliptical			
	3mm	226+647=873 Watt	
	8mm	138 Watt	420 Watt
Present Set-up			
	8mm	395 Watt	1212 Watt

10.7.3 Frequency Domain

The resonant losses from a single mode are given by

$$Powerloss = 2 \times I^2 \times Rshunt, \tag{38}$$

where I is the total beam current and Rshunt the shunt impedance for the mode.
The frequencies and resonant fields were calculated for 150 modes. Only modes with a non-zero z-component for the electric field can interact with the beam, so there was a magnetic boundary condition set at the x-z plane. Thus, for the cylindrical beam tube the frequencies of interest lie between 1.73 and 3.66 GHz and for the elliptical case between 3.8 and 5.8 GHz. The Q-values, loss parameters, shunt impedances and resonant power losses can then be obtained, see Table 36. It is a reasonable assumption that only one mode will be excited at any one time,

Table 36: Cylindrical Beam Tube: Resonant Losses for modes with Shunt Impedance $> 7 \times 10^4$

Mode	Frequency (MHz)	Q-factor	Kz (V/C)	Rshunt (Ohm)	Loss (Watt)
23	2190.613	23765	0.809080E+11	2.794E+05	2012
27	2298.455	26735	0.251644E+11	9.317E+04	671
30	2371.982	26761	0.200173E+11	7.189E+04	518
46	2552.252	26262	0.292109E+11	9.568E+04	689
69	2851.288	27133	0.377697E+11	1.144E+05	824
70	2871.136	28104	0.232426E+11	7.242E+04	521
79	2998.508	27599	0.719452E+11	2.108E+05	1518
99	3162.331	28918	0.445715E+11	1.297E+05	934
104	3201.377	30180	0.273706E+11	8.213E+04	591

so the figures given here are for the mode with the highest power loss. As the power loss for each mode has a different distribution, plots have also been produced to show the maximum expected loss from any mode at any one 10 cm segment - see Figure 83. The losses plotted in this figure cannot be summed to give the total loss, as the contributions come from different modes and will not occur simultaneously.
Fig 84 and Fig 85 show the electric field for two different modes, in the upper plot the fields are trapped on the left hand side of the interaction region, in the lower plot they are trapped between the synchrotron mask and the beginning of the elliptical beam tube on the right hand side.

10.7.4 Comparison with the present Configuration

Similar calculations were made for a change in the beam tube at the end of 1994, the configuration which is now in place. Modes were then trapped in the region from $z = -2.24\,m$ and $z = 2.5\,m$. The present calculations show an increase in single pass impedance of approximately 20% and an increase for the mode with the maximum shunt impedance of 40% for a bunch length of 8 mm.

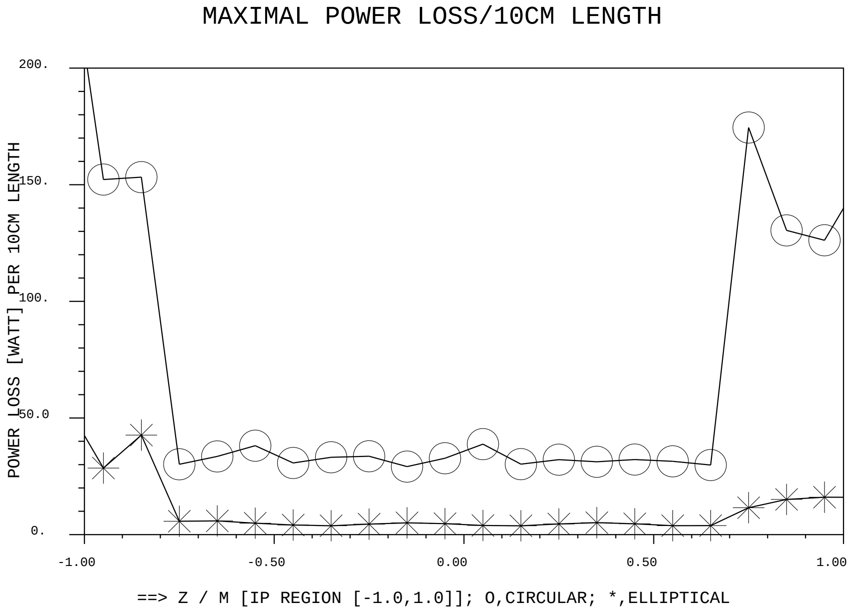

Figure 83: This plot shows the maximum possible loss from trapped modes at each 10 cm segment around the Interaction Region. The values for the circular beam tube are marked with o's and those for the elliptical beam tube with *'s.

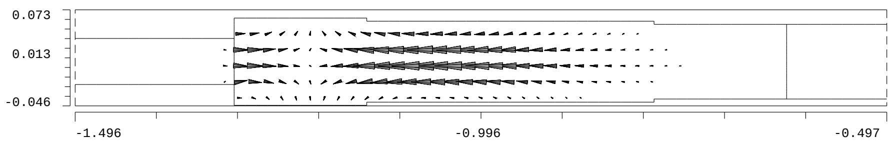

Figure 84: Electric field in the symmetry plane, y=0, for the 2.37 GHz mode.

10.7.5 Conclusion

Although the present calculations cannot be directly compared with the 1994 ones, the maximum losses occur at the beam tube constrictions in both cases. Thus one can expect at least a 20% increase in impedance over the present configuration. If the use of an elliptical instead of a cylindrical beam tube were possible this would reduce the losses considerably. The main problems are likely to occur at injection when the electron or positron bunch is shortest.

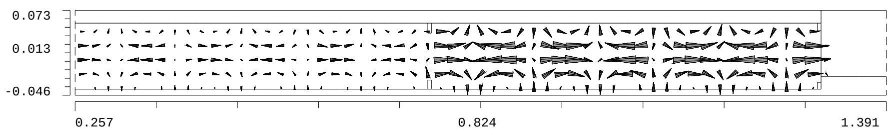

Figure 85: Electric field in the symmetry plane, y=0, for the 3.00 GHz mode.

10.7.6 Modified Geometry for Rev2 Lattice

The worst case estimation of resonant losses (table 34) and of transient losses (table 36) for the geometry in Fig. 82 leads to values in the kW range so that a strong cooling system especially in the range of the superconducting quadrupoles is needed.

This can be avoided by small changes in the geometry of the beam pipe: the resonant losses are caused by modes which are completely trapped in the part of the pipe with the largest cross-section and therefore with the lowest cutoff frequency f_c. As the power cannot propagate through the adjacent pipes with higher f_c, the quality of these modes is determined by wall losses, which leads to high Q-factors (of the order of 25000) and high shunt impedances. These values can be reduced by more than one order by coupling to waveguide modes with lower cutoff frequency. To achieve this, the symmetry with respect to the x-z-plane has to be broken slightly so that the E_{11n}-modes (e.g. in Figure 84) can couple to the H_{10} waveguide modes. This coupling mechanism and the power propagation into the beam pipe is demonstrated in Figure 86. The asymmetry can be caused the arrangement of absorbers or by an offset.

The losses of higher spectral components (e.g. above 10 GHz) are estimated by the 'single pass power loss'. This quantity describes the power loss of the beam, but only a fraction of this energy is absorbed in the walls of the interaction region. Most of the energy propagates upstream and downstream into the beam pipe and is dissipated over a great length. To minimize all reflections back to the experimental region, the Rev2 design avoids abrupt changes of the beam pipe cross-section. The intersection of absorbers can be tolerated, if their surfaces are small compared to the pipe cross-section.

References

[1] The MAFIA Collaboration, CST GmbH, Lauteschlägerstr. 38, 64289 Darmstadt, Germany.

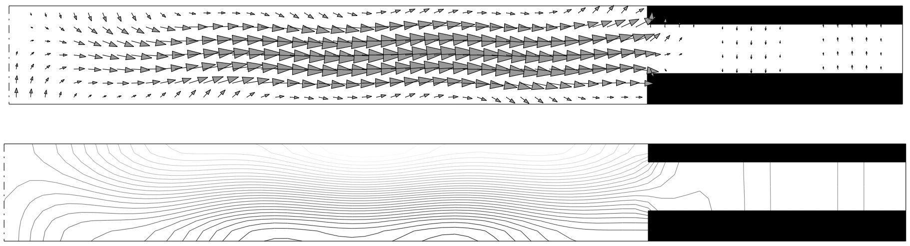

Figure 86: Electrical field in the plane x=0 for a configuration without y=0 symmetry. The 'cavity field' stimulated by the beam is partially converted into a mode which can propagate through the beam pipe.

11 Beam Position Measurements

11.1 Introduction

The planned luminosity upgrade for H1 and ZEUS will feature HERA machine focussing magnets placed within the experiments themselves and located to within 1.8 metres of the interaction points (IP) in order to reduce the beam dimensions at the IP (see section **??**). This new scheme whilst providing increased luminosity to the experiments will increase the demands placed on the machine operators in attaining and maintaining the higher luminosity whilst simultaneously minimising the experimental backgrounds.

In order to achieve the higher levels of luminosity quickly, safely and reliably the question of the monitoring of the transverse beam positions through H1 and ZEUS has to be considered. This note is intended to discuss the requirements, the problems to be tackled and possible monitoring solutions.

11.2 Constraints related to monitor operation in the interaction areas

Operation of transverse beam pickups located in the joint (e-p) beam pipe sections in the north and south HERA experimental areas will have to take into account special considerations.

- A given beam pickup will 'see' and deliver signals from both beams.
- An electrostatic monitor will also detect travelling wakefields from longitudinal higher-order modes within the beam pipe.
- The pickups must be radiation hard, present a minimal disturbance to the beams and be able to operate reliably at elevated beam pipe temperatures.

With regard to the first point we note that the delivered electron and proton derived signals from a given pickup will be separated in time depending on the z-position of the pickup with respect to the interaction point. The beams will be coincident in time at a given z position at integer multiples of 14.4 metres distance from the IPs.

Concerning the wakefields; these are most likely to be produced by the electron beam as the electron bunches are roughly an order of magnitude shorter in length than the proton bunches (3 cm compared to 30 cm total length), and therefore have much higher energy content at higher frequencies. Above the beam pipe cut-off frequency the higher-order modes can propagate freely and even below this frequency some propagation in evanescent modes is to be expected. The levels of higher-order modes excited and the frequencies at which they appear, will depend on the geometrical and RF design of the beam pipe and particularly on the type of beam pipe transitions in the area of the IPs. As noted the pickups themselves should not impinge on the beams thereby reducing beam intensity and should not themselves add significant longitudinal impedance to the machine as seen by the beams, i.e. they should not themselves create significant higher-order mode losses.

11.3 Monitoring of the Protons

Most of the experimental backgrounds are proton related and are either derived from beam-gas or beam-wall interactions. Presently the total circulating proton current is at about half of the design value. We may expect this current will approach the design value with time and as it does so the potential for proton related damage to the detectors due to missteering or machine related accidents will increase.

In order for the minimisation of the proton related backgrounds whilst operating under conditions of higher luminosity the position of the proton beam will have to be closely and accurately monitored. The required x and y position resolution is ca. $30\,\mu$m or better which would be comparable to the smallest beam size ($\sigma = 32\,\mu$m in the y-direction). Unlike the proton position monitors presently installed within HERA-p, in this new application it is not necessary to have position information stored on a turn by turn basis to be available for a post-mortem beam diagnosis. It is expected that position measurements updated at 3-5 Hz will be sufficient for a machine operator to place the beam at a given, optimal transverse position required for luminosity operation. The advantage of this relatively low update rate, is that one may use signal averaging methods to reduce noise in the measurement system and to deliver more accurate and reproducible position measurements. Furthermore an absolute position measurement of the proton beam is not required: it will be sufficient for the operator to be able to position the beam at a given x and y coordinate previously determined by the position measurement system regardless of what this position really corresponds to compared with center of the beam pipe. We note that the position accuracy delivered by a monitor is not only determined by the machine tolerances of the beam pickup itself but also on the position stability of the beam pipe into which it is installed: this latter effect will be of particular importance in the luminosity upgrade program where thermal heating effects of the beam pipe may be significant and where compromises in the beam pipe and magnet support structures inside the experiments may have to be made.

In order to provide position measurements in the region of the experimental interaction points one has to take into account the presence of the electron bunches present within the same beam pipe section. It is the presence of this second particle beam that will put the most constraints on the accuracy of the proton position monitoring. The ideal pickup for this application would itself provide filtering out of the undesired electron signal though further external filtering and processing might be necessary. Because of the shorter length of the e-bunches low-pass filtering will preferentially reduce the electron signal magnitude over that of the protons. At positions removed from z = 0 (the interaction point) the protons and electron bunches will pass the monitor at different times with respect to the HERA Bunch Clock, giving rise to the possibility of sampling the signal from the monitor at fixed times thereby exclusively deriving a proton signal. At z = -1.8 metres, at the IP end of the final focussing magnet the temporal separation between the 2 beams will be 12 ns.

This clear picture may be spoiled be the presence of wakefields in the beam pipe near the IP. These fields will be picked up by a longitudinally sensitive pickup and the resulting signals may be present at a time when protons are also passing the pickup and thus they may contaminate and degrade the sensitivity of the position measurement. From the point of view of wakefields it is highly desirable to have the proton pickup located at the -z side (proton side) of the interaction point: this would give the maximum amount of time for the wakefields from a previous e-bunch to die down before the measurement of a proton position.

For this application the best pickup for the proton beam would be a stripline or directional coupler. The advantage of this design lies in its directivity: indeed electron signals may be reduced by up to ca. -20 dB at the upstream, proton port, given good stripline design. In order to get good directivity the stripline should be as long as possible. However as the stripline length increases it becomes increasingly difficult to maintain a constant impedance (normally 50 ohms) along its length and directivity suffers correspondingly. A good compromise between signal amplitude and directivity for the protons would be a stripline length close to the proton bunch length of around 30 cm. The monitor itself would be comprised of 4 such parallel striplines spaced at 90 degrees around the beam pipe azimuth and located in an X-form (45 degrees to horizontal and vertical planes) in order to remove the striplines as far as possible from both the synchrotron radiation fan and any transverse beam tails. The exact positioning of the striplines will depend on the final beam pipe cross-section chosen but in the ideal case would be such that the centre of charge of the proton beam during luminosity is close to the geometric centre of the monitor so ensuring that the signal amplitudes delivered by the striplines are linearly proportional to the transverse beam position. Because absolute beam position determination isn't a requirement this linear response of signal to beam position is not a rigid criterion: nevertheless it would make monitor calibration significantly easier.

The striplines themselves could be machined from gold-plated copper and positioned away from the beam pipe walls using low-profile, ceramic, SMA vacuum feedthroughs such that the striplines present a characteristic impedance of 50 ohms along their lengths and present an optimal match to 50 ohm coaxial cable. There are a number of free parameters in the stripline design (width, thickness and separation from the inner beam pipe wall) which may be optimised to ensure large signal amplitudes, to maximise the stripline stiffness and free beam aperture whilst keeping the inter-stripline capacitances under control. These parameters and a detailed design to minimise the longitudinal impedance seen by the beam may be undertaken only once a beam pipe section has been chosen.

Should there however be a restriction on the longitudinal space available such that striplines of sufficient length cannot be accomodated into the new beam pipe then the alternative choice would be striplines of reduced length or even zero length striplines, better known as capacitative buttons. These devices would have no directional selectivity between protons and electrons in our application and therefore any differentiation between the two signal types would have to be done entirely electronically using devices external to the pickup. The advantages of buttons is that they are small, easy and cheap to manufacture and that they impose minimal shunt impedances to the beams and dead material to the experiments. There are 4 button pickups installed in the common e-p section of H1 and observational experience using these devices for both protons and positrons has been good.

11.3.1 Electronic Signal Analysis

The proton signals derived from the four striplines (or buttons) will be treated in the normal fashion to produce horizontal and vertical position signals independent of the proton beam intensity. There are some choices in the electronics that could be used:

The company Bergoz Precision Beam Instrumentation manufactures a beam position monitor processing card based on Jim Hinkson's design for the Advanced Light Source at LBL [1]. This unit is reported to work very well. The device accepts four signal inputs over a 75 dB dynamic range into 50 ohm inputs. The sensitivity of the device is variable and the board itself is quoted as having a $1\,\mu$m x and y resolution at 1 V/m sensitivity. This is well within our requirements. Furthermore the x and y sensitivities are variable in order to compensate for changes in the vacuum chamber cross-section. Another useful feature is that the user may set a bandpass filter in the electronics chain on the card to control and limit the bandwidth of the signals processed; with this feature we may additionally filter out electron derived signals. The unit provides three analogue output signals which could easily be digitised to incorporate the data into the existing HERA control system.

Should the level of onboard signal filtering be insufficient to sufficiently suppress residual electron derived signals then further filtering must be undertaken. This additional filtering could amount to:

1. prefiltering of each of the four input signals with low pass filters. These filters would have to be identical in response.

2. modifying the Bergoz card so that additional bandpass filtering could be installed on-board or on a daughter card. This additional bandpass filter would affect all four signals uniformly.

   One should however note that additional frequency filtering will only be of limited use in differentiating the electron and proton beam signals despite the factor of 10 difference in bunch length. If we assume a Gaussian envelopes for a given beam bunch, then in the frequency domain we also get a Gaussian response. If we now sample this response at say 500 MHz and again a frequency of 5 GHz (a factor of 10 increase), we will find that the signal amplitude has only dropped by -0.67 dB at the higher frequency. This illustrates the slow roll of of a Gaussian with frequency. Despite the short bunch length of the electrons in comparison to the protons the above arguments imply the presence of significant proton current at very high frequencies. In practice the proton will have even more high frequency energy than implied above because the bunch shape is limited in time by the finite length of the RF bucket unlike a true Gaussian distribution which is unlimited. These arguments lead us to the third processing solution:

3. filtering in time. Since the electron signals arrive at a fixed time offset compared to the protons using a fast switching unit triggered by the HERA Bunch Clock in order to time-gate out the undesired signals to a high level of suppression. This is an available option, called "Fast NIM gate", on the Bergoz modules. The gate opens and closes

GaAs switches in about 2 ns but in practice around 10 ns is needed to go from good isolation to good conduction with the same time being needed for the reverse process. This time corresponds to the flight time difference of two particle beams 1.5 meters from an interaction point so that pickups at 1.8 metres distance may have their signals effectively switched by such a gating unit. The maximum switching speed of the Bergoz electronics is 3.5 MHz and is limited by the maximum power dissipation of MOS logic. This is somewhat lower than the 10.4 MHz bunch frequency in HERA: Julien Bergoz has however indicated that the switching speed could be improved with design changes. If we were to gate on proton pilot bunches rather than on all proton bunches then no design changes would be necessary and we could even move a pickup closer to the IP.

The idea that one could process the four monitor signals in the time domain leads to another processing solution: one could simply use an oscilloscope. As previously explained, in the time domain the e and p signals will be separated in time according to the pickup's position in z along the beam pipe. A fast digitising 'scope may then be used to digitise the signals from each stripline (or button) in a given time window. Either four, 50 ohm scope channels could be used for the signal inputs or one could use a coaxial switching unit to switch each signal in turn across one 'scope input channel. The measurements here are essentially single bunch measurements but the advantage of using this approach is that one could use internal 'scope software to integrate and average the input signals over many revolutions thereby increasing the signal to noise ratio. Furthermore the system software could be used to provide the intensity independent x and y position signals. Using the HERA First Bunch Clock (rather than the Bunch Clock) as a trigger in conjunction with the internal 'scope trigger delay would allow one to selectively trigger on the proton pilot bunches and thus to minimise any baseline effects due to electron derived signals in the same way as described in the previous paragraph for the Bergoz electronics module. Whilst such a processing system would be versatile and powerful it does have a distinct disadvantage; namely cost. A suitable 'scope, such as the HP54720D, would cost roughly 80 kDM per experiment at today's prices. This compares with 4,900 DM for a Bergoz beam position monitor processing module. There is a working existence proof for using the HP54720D to look at single bunch signals delivered from a stripline monitor: the author has installed such a system into H1 for proton bunch satellite measurements which are processed over a 2 GHz analogue bandwidth at 2 GSamples per second sampling rate. One might hope that the cost of such a 'scope will fall with time as more powerful models replace it.

11.4 Monitoring the Electrons

Measuring the transverse position of the electron beam near the IP will enable the machine operators to tell when the two particle beams are aligned for luminosity operation. The position monitoring of the electrons close to the interaction region can proceed similarly to the case of the proton measurements. We note that upstream ports (now for the electrons) of any striplines installed into the common beam pipe section can be used to make electron position measurements as the proton derived signals are attenuated by up to -20 dB from these ports. For the electron signals additional bandpass filters (rather than low pass for the protons), could be applied to further increase the immunity from the residual proton signals but the previous proviso concerning the frequency spectrum of Gaussian signals still applies. In the the time domain one has to also be aware of out of time proton signals. The proton satellites, may appear at $\pm$ 4.8 ns separation from the main proton bunches at an intensity of between 0 and 10 % of them. Such residual proton signals could leak into the electron position measurements and degrade their accuracy. The amount of leakage will depend largely on the z-location of the pickup; a device exclusively devoted to an electron measurement and located between z = + 1.2 - 1.8 metres would have the maximum noise immunity from proton related signals, both those in and out of time.

Considering the electronics processing for the electron signals exactly the same arguments apply as for the protons except that any processing in the frequency domain could occur at much higher frequencies than for the protons before being limited by noise considerations.

11.4.1 Synchrotron Radiation

If anything the position measurement of the electron bunches is more critical than that of the protons. the extra focussing of the electrons will give rise to a fan of synchrotron radiation of considerable intensity which much be cleanly and safely transported down the beam pipe, out of the experimental areas and into appropriate absorbers. As the total synchrotron radiation power will be about 25 kWatts and the critical energy ca. 180 keV, the potential damage to the experiments due to misguided or scattered radiation is considerable. For this reason it is desirable to monitor the position of the synchrotron radiation itself at some point way downstream from the IP. Because the synchrotron radiation will be a rather thin Gaussian in the vertical plane and considerably broader in the horizontal plane it will be considerably easier to monitor the vertical position of the fan. It is proposed not to try to measure the horizontal position as the beam pipe section will be designed to accommodate the significant horizontal spread of the synchrotron radiation. In the vertical plane both the position and tilt of the electron beam will be critical; here one could hope to derive the tilt measurement from the e-beam position measurement taken near the IP combined with the vertical synchrotron radiation fan measurement many metres from it.

For monitoring the position of the synchrotron radiation there are two main, plausible solutions. Firstly one could apply optical methods to the radiation fan: for example by using a fixed beryllium extraction mirror to divert a vertical slice of the synchrotron radiation out of the beam pipe via a quartz window. Once outside the beam pipe the UV content of the radiation could be wavelength shifted into the visible region an directed into a CCD camera. This and similar schemes have been developed and used in many laboratories, for example at LEP by Baribaud et al. [2].

A second solution to the problem has already been implemented in the wiggler and undulator beam lines at DORIS. The radiation monitors here consist essentially of parallel tungsten plates which form an aperture for the synchrotron radiation but which also intercept a fraction of the Gaussian tails. The tungsten plates are electrically isolated from their surroundings and support structures and are water cooled. Electrical currents flowing from each plate due to photo-emission are then measured and combined to give an intensity independent position measurement in the usual way. In the DORIS monitors the output signal varies almost linearly for vertical displacements of up to $\pm$ 1 mm and the minimum detectable displacement change was 10 μm for synchrotron radiation with a critical energy of 13.7 keV.

Both monitoring schemes have their advantages and disadvantages. In the optical scheme we only require a cooled, fixed mirror in the beam pipe allowing us to make measurement adjustments outside. A typical pixel dimension in a CCD array is $12\,\mu$m and it is this number which determines the position resolution if light is shone directly onto the array. However by using a convex mirror to produce a 'light lever arm' the resolution may be increased. Care will have to be taken to minimise saturation of the CCD pixels from the light intensity and to damage resulting from presence in a high radiation environment.

The tungsten aperture system as used in DORIS has some advantages: the resolution is very good (a factor 10 better than the button pickups in DORIS), and the signal processing electronics has been developed to completion and works very well. The disadvantage with this method is that relatively small vertical displacements of the synchrotron radiation fan can increase the thermal load on one of the plates dramatically. In DORIS this problem has been solved by mechanically moving the monitor (in both x and y planes) to recentre the radiation between the plates: this requires a complicated movement and bellows assembly and considerably increases the longitudinal space required for the monitor. In HERA one could use a fixed monitor provided one were very confident about the final vertical and tilt of the e-beam for optimal luminosity; however in practice as likely as not, the best luminosity versus background conditions for the experiments will be determined empirically. Thus if this solution is adopted for HERA it would be advantageous to facilitate vertical position adjustments of the monitor.

In HERA it will be desirable to measure the synchrotron radiation position as far from the experiments as possible in order to minimise the levels of radiation scattered back into the sub-detectors and to improve the beam 'tilt' measurement accuracy. However close to the final synchrotron radiation absorbers (z = ca. - 24 metres) the levels of back scattered radiation will be high and will give rise to background currents from the tungsten plates and increase their thermal load. For a tilted absorber as much as 20 % of the radiation may be scattered. As the scattered radiation would be incident on the tungsten plates at different times compared to the direct incident radiation one could conceive of the development of an electronic switching unit to time-gate out the unwanted, backscattered signals. This would only be useful if the actual response time of the photo-emitted current measurement system is on the order of several nanoseconds. The optical method would be far less sensitive to backscattered radiation because the rear of the beryllium mirror would reflect it into the beam pipe wall rather than out of the quartz window.

A further suggestion for the synchrotron radiation monitoring would be to try to integrate the monitor with the final absorber. The absorber itself is likely to be tilted in the vertical plane in order to spread the radiation over as large an area as possible. Factors of 10 or 20 have been mentioned. The idea would be to apply a set of fine horizontal (or near horizontal) wires to a very thin, sputtered ceramic coating on the face of the absorber and to measure the photo-emission current from each wire in order to build up the profile and position of the synchrotron radiation fan. As the absorber will be cooled one might hope that the provided each wire only intercepts a small fraction of the synchrotron radiation power the wires will remain intact. It is by no means certain that this will be the case and investigative calculations need to be performed on the expected heat load versus position in the smeared radiation fan for wires or strips of varying dimension.

A variation of the above idea would be to measure the temperature gradients on the front of the absorber block directly. A linear array of platinum resistance thermometers (PRT), embedded in the tungsten absorber close to the surface could be used to read out a temperature profile. This profile could be fitted to a peak in order to determine the peak position of the synchrotron radiation profile. Commercial PRTs are available for measurement over very wide temperature ranges and with transverse dimensions down to 1 mm. If we assume 1/ a linear array of 1 mm diameter PRT probes each separated from its neighbour by 2 mm, 2/ a synchrotron radiation profile of 5 mm width at it's widest point (see section 10.5) and 3/ an absorber tilted to smear the profile in 2/ over the absorber surface by a factor of 10, then the beam would be profiled by 10 probes. The accuracy of determining the peak depends on the resolution of the PRTs and the variation of the temperature profile above the 'background' temperature; this is dependent on the thermal conductivity of the absorber block and the efficiency of it's cooling. Nevertheless it is expected that the peak of the profile can be found in any case to within better than 1.5 mm projected onto the vertical plane; this is the equivalent of 50 times the vertical sigma of the electron beam. Given that the final absorber will located at z = ca. - 24 metres this would give a resolution on the electron beam tilt of 0.06 mrads. An improvement could be made by increasing the granularity of the PRT array but in order to achieve a vertical resolution on the order of 30 μm we would have to instrument with PRT probes at 0.3 mm pitch. If the temperature profile has a low error distribution and can be well fitted by a Gaussian curve a lower sensor pitch could however give rise to the same resolution. Because of the nature of this measurement useful update rates would be on the time scale of several seconds allowing any change in the y-position of the synchrotron radiation distribution to build a new steady state temperature distribution within the cooled absorber block. This method would also be useful for measuring the synchrotron radiation position in the intermediate absorber at z = - 11 metres. The advantage of this measurement method is that it is independent of the levels of backscattered radiation and it in itself does not cause additional backscattering.

11.5 Conclusions

This preliminary report has looked at some possibilities to perform accurate beam position measurements for the planned luminosity upgrade. The problems to be tackled have been elucidated and various methods of overcoming them have been suggested. Despite the preliminary nature of this work some conclusions can be drawn:

1. The optimal beam measurement system near the IPs would use dedicated proton striplines matched to the proton bunch length at z = - 1.8 metres and shorter dedicated striplines matched to the electron bunch length at z = + 1.8 metres. The Bergoz beam position monitor cards would fulfill the signal processing requirements entirely. The e^+e^- collider DAFNE will soon be operating using beam position monitoring based entirely on Bergoz modules triggered in the fast NIM gate mode: the results of signal crosstalk measurements in practice on this collider are of great interest to us to determine the position resolution we might hope to obtain. This subject is currently under discussion with Bergoz. Additional monitoring outside of the areas possessing a common beam pipe could in comparison be trivially performed by using capacitative button pickups in conjunction with Bergoz signal processing cards without the use of fast bunch gating.

2. The simplest method to monitor the position of the synchrotron radiation at the absorbers would be to measure temperature profiles. Other methods have been discussed in the text which would deliver more accurate position information with higher update rates but at the expense of increased complexity and in some cases, increases in the levels of back scattered synchrotron radiation.

Once again the author would like to make his appreciation known for any comments, criticisms and suggestions that are forthcoming. The author would also like to acknowledge useful discussions with Julien Bergoz of Bergoz Precision Beam Instrumentation.

References

[1] see http://www.bergoz.com/

[2] G. Baribaud, C. Bovet, R. Jung et al, 'Three dimensional bunch observation in LEP', HHEAC '92, Conf. Proc. 212-214.

12 Magnet Cooling

It is possible to connect the new magnets and the changed vacuum chambers to the existing distribution tubes. The parameters for this cooling system are: The water is deionised water with a conductivity of approximately 1 mS/cm. Therefore the only possible materials are stainless steel, copper and bronze (gunmetal). The inlet water temperature is approximately $30° C$. The possible maximum pressure difference between input and output side is 7 bar. The allowed pressure for all connected elements has to be over 16 bar, because the cooling system is a so called PN 16 (German standard) - system. The maximum temperature for the magnets has to be $70° C$ to minimise the required cooling water.

With this assumptions it is possible to cool down a additional power of roughly 500 kW per HERA hall. All magnets will be connected in parallel to the distribution tube. If the demand pressure difference of the magnet is less than 7 bar, there will be a fitting with an orifice. The vacuum chambers will be connected in series until the maximum water temperature is $70° C$. The pressure difference has usual to fit with an orifice too. To control the water flow through magnets with a power of more than 20 kW there will be a flow meter in the return water line. This measuring device is only a switch and causes a pressure loss of approximately 0.35 bar. It could be necessary to have some changes in the maintubes, because there is not any more a lot of reserve in the water cooling system. Changing the main water distribution in the hall west would save the pump power which is necessary for cooling the new magnets.

13 Surveying of IR Magnets

Surveying and alignment of the magnets QJ and QI can be carried out by using conventional methods.

For the control measurements necessary for the components inside the detector we propose to install a laser system consisting of a semiconductor laser diode connected to collimator optics via optical fiber and semi-transparent optical sensors, which have been developed by MPI München [1]. The sensors attached to the QJ and QI-magnets define the straight reference lines with respect to the HERA-accelerator. All the other components, which are equipped with sensors, can be referenced to that lines by the appropriate sensor readings. Since the magnets on the right hand side of the detector are planned to be larger than those on the left hand side it seems not to be possible to read all sensors from both laser stations. Instead we have to position the lasers in such a way that on either side a maximum of sensors can be covered. To make that feasible it may be necessary to fit the shape of the magnets according to the geodetic conditions. Additionally it could be advantageous to have a hole inside the vertex detector such that the laser beam from the left hand side can at least reach one sensor of the first magnet on the right hand side, so that the two measurements from left and right can be compared and controlled.

The described two laser beams define only two axes for positioning. To get informations on the roll of the components one has to install additional laser systems on both sides. That means that the corresponding space to install additional sensors has to be taken into account in the magnets design.

References

[1] B. Blum et al., NIM A377 (1996) 404-408.

14 Schedule